Modeling, Development and Testing of a Small-Scale Collins Type Cryocooler

C.L. Hannon[1], B. Krass[1], J. Gerstmann[1], G. Chaudhry[2], J.G. Brisson[2] and J.L. Smith Jr.[2]

[1]Advanced Mechanical Technology, Inc.
Watertown, MA, USA 02472

[2]Massachusetts Institute of Technology
Cambridge, MA, USA 02139

ABSTRACT

A multistage 10 K cryocooler is under development that is based upon a novel modification of the Collins cycle, a cycle commonly used in many large-scale high-efficiency cryogenic machines. This cryocooler design achieves its compactness and reliability by using microelectronics to enable complex valve timing in a mechanically simple yet efficient cold head design. This cycle is well suited to cryocoolers operating in a temperature range from 4 K up to 30 K. The modular nature of this design enables the configuration of application specific two-stage (30 K), three-stage (10 K), and four-stage (4 K) cryocoolers. Design innovations include floating piston expanders and electromagnetic smart valves, which eliminate the need for mechanical linkages and reduce the input power, size, and weight of the cryocooler in an affordable modular design. A sophisticated LabView based control algorithm enables electronic control of the expansion cycle. Software based control enables variable valve timing and adaptive control logic. An engineering prototype has been built that integrates a floating piston expander and recuperative heat exchanger as a functional cryocooler stage. This prototype cryocooler stage has been tested in two configurations. Initial testing was as a balanced flow single stage cryocooler. The second configuration represented the third (lowest temperature) stage of a three-stage 10 K cryocooler. In this configuration, a precooling stream was added to the low temperature side of the heat exchanger to create the unbalanced flow condition that characterizes the Collins cycle. This paper will review the engineering prototype design, the analytical modeling results, the prototype development testing, and the future development.

INTRODUCTION

Cryogenic cooling to temperatures below 30 K is required for many medical, scientific, military, and industrial applications. Magnetic Resonance Imaging (MRI) machines employ superconducting high-field magnets that require cooling to about 4 K, often by the use of liquid helium. Nuclear Magnetic Resonance (NMR) spectroscopy machines (similar to MRI machines), used to study the physical, chemical, and biological properties of matter, have similar cooling requirements. Primary voltage standard systems using superconducting Josephson Junction circuits are commonly supplied with liquid helium dewars for cooling. Military space applications include cooling infra red focal plane arrays. Current infra-red focal plane arrays (IRFPA) technology requires cooling to about 35 K, but emerging arsenic doped silicon (Si:As)

Cryocoolers 14, edited by S.D. Miller and R.G. Ross, Jr.

focal plane arrays (FPAs) will require 10 K cooling. Optical memory and processing technology, such as S2CHIP, can provide instantaneous processing bandwidth of 20 GHz when cooled to about 4K. This enables real-time signal processing for high resolution range-Doppler radar imaging, and other high bandwidth signal processing applications.

In many cases, sub-30 K cooling is provided by evaporating liquid helium supplied from a dewar. In some cases, mechanical cryogenic refrigerators (cryocoolers) are used to recondense most of the helium vapor to extend the life of the liquid helium supply. Periodic replenishment of the liquid helium is still required. Large-scale cryogenic machines used in the production of liquid helium; are generally based on the Brayton or Collins cycles.

Collins cycles routinely operate with input power of about 740 W per W of refrigeration, which is only 10 times the ideal Carnot efficiency at 4.2 K. Small commercially available Gifford-McMahon (G-M) type Stirling and pulse tube cryocoolers capable of about 1 W of cooling at 4.2K have been available for several years (Daikin, Aisin Seiki, Cryomech, Sumitomo, Leybold). These devices typically require about 5 kW - 8 kW per watt of cooling at 4.2K[1], which is about 70 to 100 times the Carnot requirement. This vast difference in performance provides the motivation behind an effort to develop a small-scale cryocooler based on the Collins cycle.

MODIFIED COLLINS CYCLE CRYOCOOLER

The Collins cycle employs a single stack of heat exchangers to cool compressed helium gas in a multistage process. A portion of the high-pressure gas stream is split from the main flow and cooled by expansion to a lower pressure. This cooled gas joins the low-pressure stream returning from the next lower temperature stage. The combined low-pressure streams cool the remaining portion of the high-pressure stream to close to the exit temperature of the expander. This effect reduces the temperature difference in the heat exchanger to a pinch point where the two low-pressure streams join at the exit temperature of the expander. Expanding a portion of the gas in successive stages allows the heat exchanger surface to be concentrated in the lowest temperature heat exchangers where it is most effective in improving the performance of the refrigerator.

The modified Collins cycle cryocooler configuration differs in that the stages are arranged in parallel, rather than in series. In this configuration the high-pressure stream is split at room temperature into substreams for each stage. A 3-stage 10 K cryocooler is illustrated schematically and as a solid model in Figure 1. A heat exchanger for each stage precools the high-pressure sub-stream to the inlet temperature for the expander of that stage. Except in the coldest stage, the exhaust stream from the expander is split. The larger portion of the exhaust stream returns through the low-pressure passage of the heat exchanger of that stage, and the smaller stream flows to the low-pressure side of the heat exchanger of the next colder stage to enhance the precooling of that stage. When multiple precooling stages are employed in this manner, the final stage is very effectively precooled, with the majority of its cooling power available to cool the load and a smaller fraction required to absorb heat exchanger losses.

Each stage of the modified Collins cycle is of nearly identical construction, consisting of a floating piston expander with an integral recuperative heat exchanger. The only difference between the stages is the overall length, which is dictated by the heat transfer surface required by the stage. The warm-end of all stages is at the same temperature, so in general, the relative length of a stage is related to its cold-end temperature.

As arranged in Figure 1, cooling is available at 77 K for the first stage, 30 K for the second stage, and 10 K for the third stage. If a fourth stage is present, 4 K cooling is available. The modular nature of this design enables the configuration of application-specific two-, three-, and four-stage cryocoolers.

A thermodynamic model has been developed to predict the performance of the modified Collins cycle operating at 10 K. The model accounts for finite component efficiencies and process stream temperature differences. It has been predicted that the modified Collins cryocooler will require 1-2 kW of electrical power to provide 2 W of cooling at 10 K (depending on the compressor efficiency). It is expected that the cold head of a modified Collins cycle cryocooler capable of 1-2 W of cooling at 10 K would be about the same size and weight as that of a G-M cryocooler of similar capacity, but would consume only 1/3 to 1/6 the power required by a G-M cooler. The compressor is expected to be proportionally smaller. Another significant advantage of the modified Collins cryocooler is that, as a DC-flow cooler, the "cold finger" does

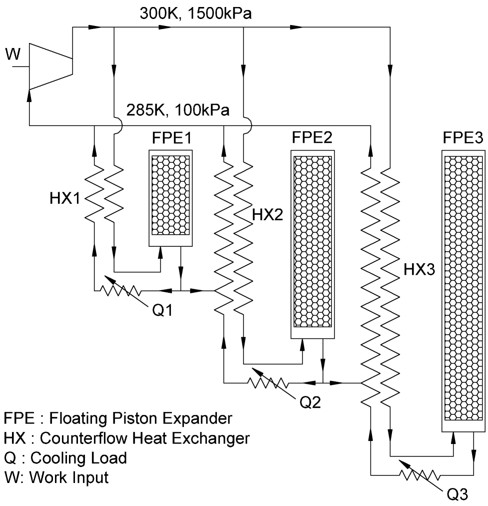

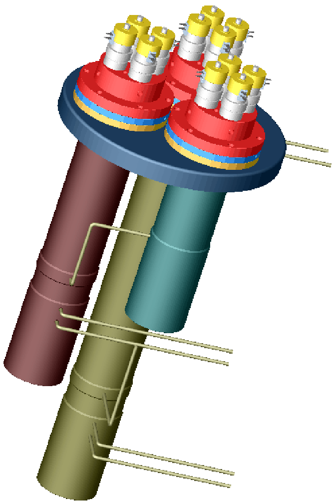

Figure 1. Schematic and 3D Rendering of Modified Collins Cycle Cryocooler

not need to be in direct contact with the cooling load. Cold helium gas can be "piped" to a heat exchanger in contact with the load. A single cryocooler could easily serve several distributed loads. This improves system integration, thermal transport, and vibration isolation.

A conventional large-scale Collins helium liquefier employs valves at the cold-end of the expander that are actuated by mechanical linkages. While these linkages act as a thermal leakage path from ambient to the 4.2 K cold-end, the magnitude of the heat leak can be made acceptably small in a large-scale machine. This becomes more difficult as a conventional Collins liquefier is scaled down to capacities less than several watts. The modified Collins cycle enables the high efficiency of the Collins cycle at a small scale by the use of the floating piston expander, which is illustrated in Figure 2. The floating piston expander prototype is also illustrated.

The expander consists of a piston (or displacer) that floats with the gas in a closed cylinder. Piston motion is controlled by electromagnetically actuated valves that require no mechanical valve linkages or

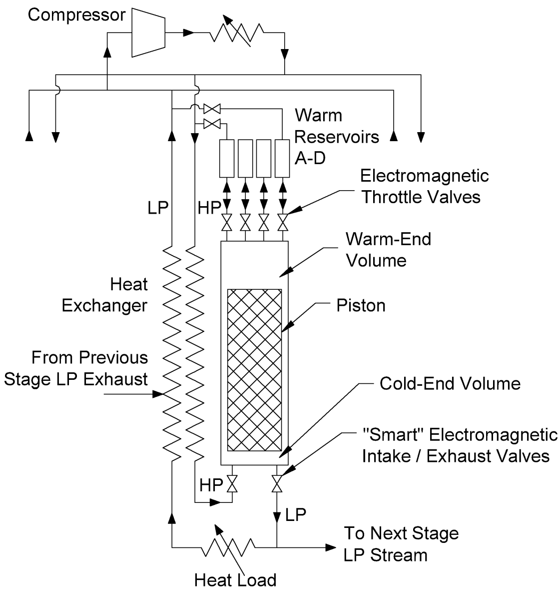

Figure 2. Floating Piston Expander

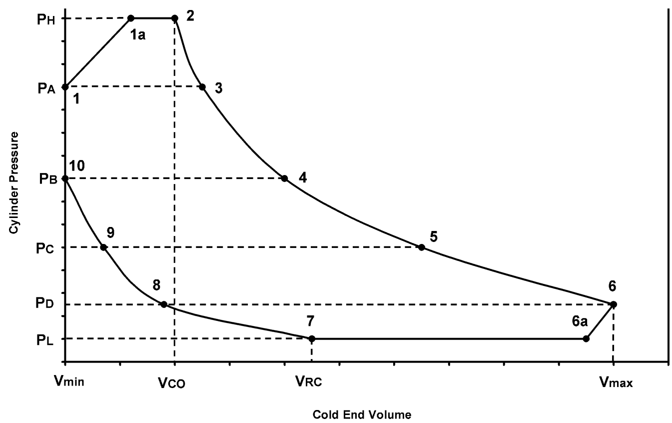

Figure 3. Ideal PV Diagram

mechanical timing mechanisms. This further reduces system complexity and improves reliability. Expander power is dissipated in the warm-end of the cryocooler using valved throttles connecting to a series of intermediate pressure reservoir volumes. A microprocessor controls the opening and closing of these valves to achieve efficient expansion of the cold gas, and to minimize losses in the cold valves.

The warm-end valves are flow-control throttling valves that control the velocity of the floating piston by controlling the rate of gas flow between the warm-end cylinder volume and the reservoirs. With this configuration, the helium pressure on the warm-end of the piston is essentially the same as the pressure on the cold end. The piston floats quasi-statically between the gas in the cylinder at the cold end and the gas at the warm end, with low velocities set by the throttling of the gas in and out of the warm-end cylinder volume. Electrical energy dissipation is minimized at the cold-end by applying only a brief high-current pulse to open the intake and exhaust valves, followed by a much lower current level to hold the valves open for the duration of the intake or exhaust event.

An ideal PV diagram for the expander is shown in Figure 3. The cycle starts at state 1. The intake process is from state 1-2, with the intake blow-in from 1-1a. Gas expansion occurs between states 2 and 6, with warm-end gas ported sequentially into reservoirs A through D. The exhaust process is from state 6-7, with the exhaust blow-down from 6-6a. Recompression is between states 7 and 1 with gas ported into the warm end volume sequentially from reservoirs D through A. Further detail on the design and operation of the floating expander can be found in other papers by the authors.[2,3]

Cycle Modeling[4]

In order to determine appropriate operational parameters for control of the floating piston expander, models were developed for all the processes that make one expander cycle. The models assumed the working fluid to be an ideal gas. It was assumed that all the processes went to equilibrium. Since the piston freely floats between the warm and cold volumes, it was also assumed that the pressure in both volumes was equal, except when the piston was flush against the top or the bottom of the cylinder. Thermodynamic models of each process were developed to evaluate the temperature, pressure, volume and mass in the warm and cold volumes at every state. The properties of each state were determined in terms of the properties of the preceding state. For steady-state operation of the expander, there must not be any net flow of mass into or out of any of the four reservoirs. This was needed to ensure that each of the reservoirs stay at the same pressure throughout the operation. The cycle high and low pressures as well as the cold end and warm end clearance volumes do not change. If the intake cutoff and recompression volumes were kept at a constant level, the cycle will consistently repeat itself.

The solution of the steady-state model depends on the values of six controllable parameters, the pressures in each of the four reservoirs, the cutoff volume and the recompression volume. Since the total mass of the gas in the four reservoirs and the warm volume is fixed, setting the net mass flow equal to zero for any three of the reservoirs will ensure that the net mass flow is equal to zero for the fourth reservoir, since the warm volume returns to the same initial state after every cycle. While there are six parameters, there are only four constraints for an ideal expander cycle in steady state. Therefore, the values of the cutoff and recompression volumes are fixed and the equations are solved to get values of the four reservoir pressures. This is done for different values of inlet pressure.

A solution does not exist for all values of cutoff and recompression volumes. It is observed that while solutions can be found for a large range of recompression volumes, the corresponding range for cutoff volumes is much smaller.

Feasible intake cutoff volumes range from 0.194 to 0.321 at a pressure ratio of 15, and from 0.179 to 0.331 at a pressure ratio of 10 (Volumes are expressed as a fraction of the swept volume). This calculated limitation on feasible intake cutoff volumes is observed experimentally.

The initial reservoir pressures are given values that were slightly different from the values required for steady-state operation to analyze the stability of the cycle. It is observed that if the reservoir pressures are not identical to their theoretical values for an ideal cycle, the system adjusts the warm-end reservoir pressures to ultimately obtain a steady state. It is also observed that no matter what the individual reservoir pressures are, the system comes to the same steady state if the sum of the pressures in the four reservoirs is the same. This result led to an important conclusion. The total mass in the warm end is directly proportional to the sum of the pressures in the four reservoirs.

Thus, it can be concluded that the only independent variables that affect the steady state operating conditions are the cutoff volume, the recompression volume, and the total mass in the warm end. This conclusion was supported by experimental data.

The steady-state model proved to be a very useful tool to set the operating parameters of the LabView control program. In addition to setting the cutoff and recompression volumes and the reservoir pressures, there were switching parameters associated with each step of the expansion cycle. Optimum values of these parameters were estimated using the steady-state model which enabled rapid tuning of the prototype expander.

However, the steady-state models did not adequately describe the performance of the expander. They assumed the thermodynamic processes that make up the expander cycle to be quasi-static. These models were improved by incorporating the dynamics of the piston motion and the fluid flow through the warm and cold volumes. Blow by past the piston was determined to be negligible in comparison to other flow rates in the expander, so it was not incorporated into the model.

A program was written in Matlab to simulate the dynamic performance of the expander. Since the flow rates and piston speed depend on pressures and temperatures that are constantly changing, each of the 12 cycle processes was broken up into a series of steps taking place over small time intervals. The intervals were small enough to ensure that the properties in the warm end and cold end could be assumed to be constant over that step. The smaller steps associated with a particular process are repeated until the condition for switching from the current process to the next process is fulfilled. The switching conditions are the same as the ones used in the LabView control routine.

The Matlab program was designed to analyze the expander at a particular cold-end temperature. Therefore, the cold end temperature must be specified along with certain other cycle constants (compressor inlet pressure, compressor exit pressure, switching condition constants, warm-end reservoir temperature) before running the expander loop. The average heat exchanger temperature is required to calculate the flow-rate through the high-pressure passages. A simulated P-V diagram is shown in Figure 4 along with an experimental P-V diagram. The simulated P-V diagram shows the performance at both the warm and cold ends, while the experimental diagram shows data for the warm end only. The P-V diagram obtained from the program is very similar to experimentally observed P-V diagrams. The one major difference is the 'waviness' seen in the warm-end pressure during the expansion and recompression processes.

The simulation helped explain the behavior of the expander during the exhaust and the first recompression processes. The P-V diagrams obtained during experiments showed that the warm-end pressure continued to decrease when the piston was past the recompression volume. It had previously been assumed that the reason for this was a delay in closing the exhaust valve. However, the simulation results indicated that this was not the case. In Fig. 4, it can be seen that the warm end pressure keeps decreasing past the recompression volume, just like in the experiments. It can also be seen that the cold end pressure starts increasing as soon as the recompression volume is hit. During the final stages of the exhaust, the

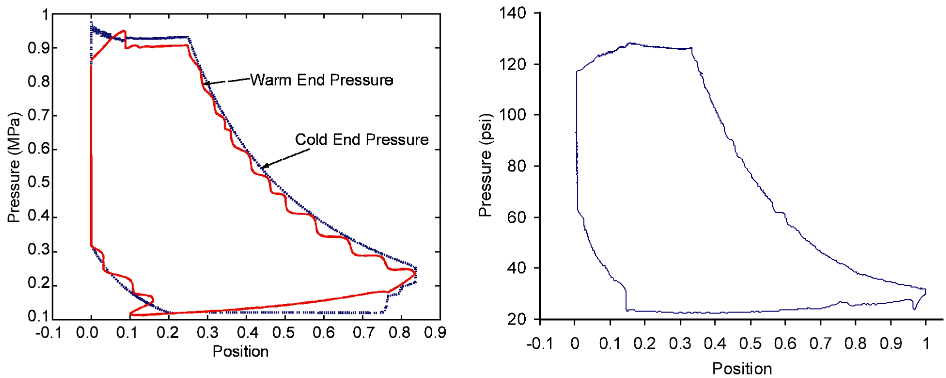

Figure 4. Simulated (left) and Experimental (right) PV Diagrams.

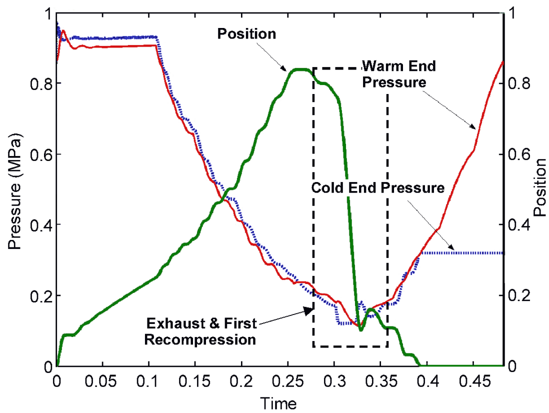

Figure 5. Simulated Pressure and Piston Position vs Time

piston has a large downward velocity (Fig. 5) as a result of the high pressure differential across it in the early stages of the exhaust. The rapid descent of the piston prevents the warm end pressure from rising even after the cold exhaust valve has closed. It was only feasible to instrument the warm-end volume with a pressure transducer, and the cold-end pressure was assumed to be fairly close to that of the warm-end volume. The dynamic simulation demonstrated that this is largely true during the expansion and recompression processes, but that significant deviations occur during intake and exhaust.

It had also been noted that the piston moved up during the first recompression. Prior to developing the dynamic simulation it had been assumed that this was due to leaks past the cold intake valve which were driving the cold volume pressure up. However, the dynamic model proved that this was a consequence of the high piston velocity during exhaust. As soon as the exhaust valve is closed, the pressure in the cold volume begins to rise rapidly. The high downward piston velocity, which prevents the warm volume pressure from rising, is also responsible for the sharp rise in cold volume pressure. This leads to a brief, but large, upward pressure differential across the piston. The large pressure differential causes the downward moving piston to decelerate and then briefly accelerate upwards. The upward motion results in an expansion of the gas in the cold end. At the same time, the flow from reservoir D into the warm end, as well as the upward moving piston, cause the warm end pressure to increase. After a few milliseconds, the pressure differential is reversed. The piston changes direction again and starts moving downwards to complete the remainder of the recompression processes.

PROTOTYPE PERFORMANCE

To demonstrate the feasibility of the cycle, a floating piston expander was designed and built that would act as the lowest temperature stage of a 3-stage 10 K cryocooler. The effect of precooling by the upper stages was simulated by adding 30 K helium gas to the low-pressure side of the heat exchanger. Changing the amount of helium being boiled off controlled the temperature of the precooling stream. If the amount of helium being boiled off was greater than the desired precooling flow rate, the excess helium was vented. The added helium was bled from the system upstream of the compressor. A schematic of the test is illustrated in Figure 6.

Prior to running tests with precooling, a series of tests were conducted with the heat exchanger in balanced flow. The expander cooled to increasingly lower temperatures as various leakage issues were addressed and as improvements were made to the cold-end valve seats. In a test that reached a terminal temperature of 107 K, it was demonstrated that the cooling rate at about 150 K was twice the cold end heat leak. Ultimately the expander was demonstrated to cool to 77 K in a balanced flow configuration, this was the expected performance for the expander in balanced flow.

In the test with precooling, the expander was first cooled to its ultimate no-load temperature in the balanced flow condition. A no-load temperature of 60 K was achieved with no precooling flow supplied. In the first experiment, the temperature of the precooling flow was set around 10 -12 K. The expander also cooled down to about 10 K-12 K. There were large fluctuations in the temperatures and it was not possible to conclude whether there was any significant cooling by the expander at this temperature. However, the system was observed to operate at these temperatures (albeit very slowly, at around 0.1 Hz), proving that the electromagnetic valves at the cold end function at 10 K.

The reason for the low cycle rate of the expander was a large leakage flow at the cold end of the expander. The leaks, coupled with a significant pressure drop across the high pressure side of the heat exchanger, prevented the pressure in the cold-end plenum from building up, with the result that the blow-in and intake strokes took a long time to complete. The desired pressure at the end of the intake stroke had to be significantly reduced (from about 140 psi at 300 K to about 100 psi) in order to keep the cycle operational. Even after this decrease, the blow-in and intake strokes took about 10 seconds to complete (as compared to about 100 milliseconds at 300 K). The remainder of the cycle took about 600 milliseconds, only slightly greater than the 400 milliseconds at 300 K. Under these conditions it was unlikely that the expander would produce enough cooling to overcome the heat leaks into the cold end.

The temperature of the helium from the dewar was increased to 30 K. At this temperature, leak rates were smaller and the expander could be cycled at a rate of about 0.25 – 0.3 Hz. The pressure at the end of the intake stroke was also higher, about 115 psi. At these conditions, the rate of expander work was significantly higher than at 10K and cooling was observed. At steady state, the temperature at the cold end was about 20K. In this test, the high-pressure flow rate was about 24 slm and the precooling flow rate was about 4% of the high-pressure flow. This compares to the design high-pressure flow rate of 32 slm and 5% precooling flow.

Prototype Performance Assessment

A condensed version of the dynamic simulation model was used to analyze the effect of the heat exchanger configuration, the plenum chamber size, and cold-end leaks on the duration of the blow-in and

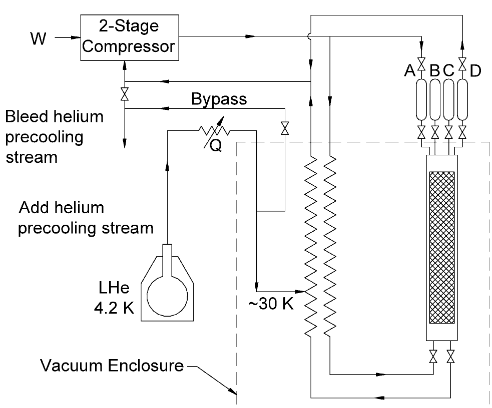

Figure 6. Schematic of Prototype Test Rig

intake strokes at various temperatures. Only the blow-in and intake processes were retained in the program. Experiments had shown that the time associated with the remainder of the cycle stayed more-or-less constant around 500-600 milliseconds. The program was run at two different cold-end temperatures, 300 K and 100 K. A compressor discharge pressure of 10 atm. was used for the simulation. The pressure in reservoir A was set to 9 atm. The cycle constants for the blow-in and intake strokes were very close to the actual parameter values used in the experiments. None of the other constants were required for this program as the blow-in and intake stroke timings are only affected by the pressure in reservoir A and the pressure in the cold-end plenum at the beginning of the blow-in.

At 300 K, the predicted blow-in/intake stroke time was about 130 milliseconds. It increased to 250 milliseconds at 100 K. The change was not nearly as drastic as that observed during experiments, even though it did suggest deteriorating heat exchanger performance. To ascertain the effect of leaks on stroke timings at low temperature, leak rates of the order of those observed at about 110 K (~4 slm) were incorporated into the model. With leak rates, the blow-in/intake time only increased to about 400 milliseconds. In the final tests, blow-in/intake stroke durations of about 450 milliseconds were observed at 100 K.

Next, the effect of increasing the number of heat exchanger coils on the blow-in/intake stroke durations was studied. Assuming a 4 slm leakage, it was found that increasing the number of heat exchanger coils from 2 to 4 resulted in a huge decrease in the intake duration at 100 K, from 400 milliseconds to 115 seconds. In the absence of leaks, it decreased from 250 msec to 105 msec.

In the next series of simulations, the effects of increasing the size of the cold-end plenum were studied. Doubling the plenum volume reduced the intake duration from 400 msec to 330 msec with leakage, and from 250 msec to 170 msec without leakage. Quadrupling the volume reduced the intake duration to 250 msec and 100 msec, respectively, for the leakage and no-leakage cases.

With leakage reduced, the effect of quadrupling the plenum volume was greater than the effect of doubling the heat exchanger coils. This was not the case with leakage included in the analysis. These results indicate that the heat exchanger impedance is not a limiting factor at temperatures of about 100 K if leak rates are kept within reasonable limits. Although doubling the number of heat exchanger coils will make a significant difference to the expander work rate, it will cut the NTU in half and increase heat exchanger losses. Increasing the plenum volume, on the other hand, will increase the expander work rate while keeping heat exchanger losses low.

CONCLUSIONS

This project has demonstrated the potential of a three-stage modified Collins cycle cryocooler to provide cooling at temperatures on the order of 10 K. The lowest temperature stage of a three-stage cooler was demonstrated, with the precooling effect of the upper stages simulated with low temperature helium gas obtained from a dewar of liquid helium. Since all three stages are of identical operation, except for overall length, demonstration of the single-stage prototype as the third stage of a three-stage cryocooler demonstrates all critical aspects of the multistage design except for control of a multistage cryocooler. Specific achievements include:

- The prototype was demonstrated to operate with the cold-end cooled to 10 K.
- A cold-end temperature of 20 K was achieved with the stage supplied with the design-point precooling flow (30 K gas at a mass flow rate of about 5% of the total system flow). Lower temperatures could not be reached due to the excessive heat load caused by cold-end leakage. Leakage past static seals at the cold end of the prototype stage was a problem throughout the project, and limited the ultimate low-temperature performance of the prototype. However, a revised cold-end configuration has been developed that will eliminate much of the clearance volume associated with the current design while providing for robust cold-end sealing.
- The floating piston expander was demonstrated to have high efficiency despite having larger clearance volume than desired.
- The electromagnetic actuators for the cold-end intake and exhaust valves worked reliably at temperatures as low as 10 K. Cold-valve sealing at low-temperature was only marginally acceptable, but insight gained from the experimental program has lead to valve design changes that will improve

sealing performance in future prototypes.

- A reliable, robust LabView based control program was demonstrated that provided deterministic control of the cryocooler cycle.
- Sophisticated analytical models of the cryocooler processes were developed that provided insight into the thermodynamics of the cycle.

While various development problems with the single-stage prototype prevented demonstration of a three-stage cryocooler, there were no fundamental thermodynamic or mechanical obstacles identified that would prevent successful development of a multistage modified Collins cycle cryocooler. Several mechanical problems with the current prototype were identified, but all can be addressed through relatively straightforward design changes. The recommended design changes reduce the complexity of fabrication and assembly, which should result in a more robust design.

The most significant technical effort required to successfully demonstrate a multistage cryocooler is the development of a control system that can coordinate and control the operation of the various stages to achieve desired operating objectives, such as rapid cooldown or high efficiency operation. The first step toward such a control system is the development of a complete dynamic system simulation to model the integrated dynamics of multistage operation. The control system and analytical models developed as part of the present work are the starting points for such a simulation.

The recommended approach toward demonstration of a multistage cryocooler follows parallel paths of analytical modeling and simulation development, and incremental validation of recommended hardware design changes. This is followed by fabrication and assembly of a three-stage cryocooler prototype, development of a multistage control system, and demonstration of high-efficiency, low-temperature cooling.

ACKNOWLEDGMENTS

This research has been sponsored by the U.S. Missile Defense Agency through AFRL Contract FA9453-03-C-0208.

REFERENCES

1. CILTEC Cryocooler Database, Center for Interfacing Low-Temperature Electronics and Coolers, (http://www.ciltec.org).
2. C.L. Hannon, B.J. Krass, J. Gerstman, G. Chaudry, J.G. Brisson and J.L. Smith Jr., "Development of a Small-Scale Collins-Type 10K Cryocooler for Space Applications," *Cryocoolers 13*, Kluwer Academic/Plenum Publishers, New York (2005), pp. 41-50.
3. C.L. Hannon, B.J. Krass, J. Gerstman, G. Chaudry, J.G. Brisson and J.L. Smith Jr., "Development and Testing of a Small-Scale Collins-Type Cryocooler," *Adv. in Cryogenic Engineering*, Vol. 51B, Amer. Institute of Physics, Melville, NY (2006), pp. 1877-1884.
4. G. Chaudhry, "Modelling of a Floating Piston Expander Employed in a 10K Cryocooler," Master's Thesis, Massachusetts Institute of Technology, September 2005.